

---

# HiFi-GAN: Generative Adversarial Networks for Efficient and High Fidelity Speech Synthesis

---

**Jungil Kong**  
 Kakao Enterprise  
 henry.k@kakaoenterprise.com

**Jaehyeon Kim**  
 Kakao Enterprise  
 jay.xyz@kakaoenterprise.com

**Jaekyoung Bae**  
 Kakao Enterprise  
 storm.b@kakaoenterprise.com

## Abstract

Several recent studies on speech synthesis have employed generative adversarial networks (GANs) to produce raw waveforms. Although such methods improve the sampling efficiency and memory usage, their sample quality has not yet reached that of autoregressive and flow-based generative models. In this study, we propose HiFi-GAN, which achieves both efficient and high-fidelity speech synthesis. As speech audio consists of sinusoidal signals with various periods, we demonstrate that modeling periodic patterns of an audio is crucial for enhancing sample quality. A subjective human evaluation (mean opinion score, MOS) of a single speaker dataset indicates that our proposed method demonstrates similarity to human quality while generating 22.05 kHz high-fidelity audio 167.9 times faster than real-time on a single V100 GPU. We further show the generality of HiFi-GAN to the mel-spectrogram inversion of unseen speakers and end-to-end speech synthesis. Finally, a small footprint version of HiFi-GAN generates samples 13.4 times faster than real time on CPU with comparable quality to an autoregressive counterpart.

## 1 Introduction

Voice is one of the most frequent and naturally used communication interfaces for humans. With recent developments in technology, voice is being used as a main interface in artificial intelligence (AI) voice assistant services such as Amazon Alexa, and it is also widely used in automobiles, smart homes and so forth. Accordingly, with the increase in demand for people to converse with machines, technology that synthesizes natural speech like the human speech is being actively studied.

Recently, with the development of neural networks, speech synthesis technology has made a rapid progress. Most neural speech synthesis models use a two-stage pipeline: 1) predicting a low resolution intermediate representation such as mel-spectrograms (Shen et al., 2018, Ping et al., 2017, Li et al., 2019) or linguistic features (Oord et al., 2016) from text, and 2) synthesizing raw waveform audio from the intermediate representation (Oord et al., 2016, 2017, Prenger et al., 2019, Kumar et al., 2019). The first stage is to model low-level representations of human speech from text, whereas the second stage model synthesizes raw waveforms with up to 24,000 samples per second and up to 16 bit fidelity. In this study, we focus on designing a second stage model that efficiently synthesizes high fidelity waveforms from mel-spectrograms.

Various studies have been conducted to improve the audio synthesis quality and efficiency of second stage models. WaveNet (Oord et al., 2016) is an autoregressive (AR) convolutional neural network that demonstrates the ability of neural network based methods to surpass conventional methods in quality.

However, owing to the AR structure, WaveNet generates one sample at each forward operation; it is prohibitively slow in synthesizing high temporal resolution audio. Flow-based generative models are proposed to address this problem. Because of their ability to model raw waveforms by transforming noise sequences of the same size in parallel, flow-based generative models fully utilize modern parallel computing processors to speed up sampling. Parallel WaveNet (Oord et al., 2017) is an inverse autoregressive flow (IAF) that is trained to minimize Kullback-Leibler divergence from a pre-trained WaveNet called a teacher to it. Compared to the teacher model, it improves the synthesis speed to 1,000 times or more, without quality degradation. WaveGlow (Prenger et al., 2019) eliminates the need for distilling a teacher model, and simplifies the learning process through maximum likelihood estimation by employing efficient bijective flows based on Glow (Kingma and Dhariwal, 2018). It also produces high-quality audio compared to WaveNet. However, it requires many parameters owing to its deep architecture with over 90 layers.

Generative adversarial networks (GANs) (Goodfellow et al., 2014), which are one of the most dominant deep generative models, have also been applied to speech synthesis. Kumar et al. (2019) proposed a multi-scale architecture for discriminators operating on multiple scales of raw waveforms. With sophisticated architectural consideration, the MelGAN generator is compact enough to enable real-time synthesis on CPU. Yamamoto et al. (2020) proposed multi-resolution STFT loss function to improve and stabilize GAN training and achieved better parameter efficiency and less training time than an IAF model, ClariNet (Ping et al., 2018). Instead of mel-spectrograms, GAN-TTS (Bińkowski et al., 2019) successfully generates high quality raw audio waveforms from linguistic features through multiple discriminators operating on different window sizes. The model also shows fewer FLOPs compared to Parallel WaveNet. Despite the advantages, there is still a gap in sample quality between the GAN models and AR or flow-based models.

We propose HiFi-GAN, which achieves both higher computational efficiency and sample quality than AR or flow-based models. As speech audio consists of sinusoidal signals with various periods, modeling the periodic patterns matters to generate realistic speech audio. Therefore, we propose a discriminator which consists of small sub-discriminators, each of which obtains only a specific periodic parts of raw waveforms. This architecture is the very ground of our model successfully synthesizing realistic speech audio. As we extract different parts of audio for the discriminator, we also append a module to the proposed generator that places multiple residual blocks, each of which observes patterns of various lengths in parallel.

HiFi-GAN achieves a higher MOS score than the best publicly available models, WaveNet and WaveGlow. It synthesizes human-quality speech audio at 3.7 MHz on a single V100 GPU. We further show the generality of HiFi-GAN to the mel-spectrogram inversion of unseen speakers and end-to-end speech synthesis. Finally, the tiny footprint version of HiFi-GAN requires only 0.92M parameters while outperforming the best publicly available models and the fastest version of HiFi-GAN samples 13.44 times faster than real time on CPU and 1,186 times faster than real time on single V100 GPU with comparable quality to an autoregressive counterpart.

Audio samples are available on the demo web-site.<sup>1</sup> We will make the implementation publicly available soon for reproducibility and future study.

## 2 HiFi-GAN

### 2.1 Overview

HiFi-GAN consists of one generator and two discriminators: multi-scale and multi-period discriminators. The generator and discriminators are trained adversarially, along with two additional losses for improving training stability and model performance.

### 2.2 Generator

The generator is a fully convolutional neural network. It uses a mel-spectrogram as input and upsamples it through transposed convolutions until the length of the output sequence matches the temporal resolution of raw waveforms. Every transposed convolution is followed by a multi receptive field fusion (MRF) module, which we describe in the next paragraph. Figure 1 shows the architecture

---

<sup>1</sup><https://jik876.github.io/hifi-gan-demo/>

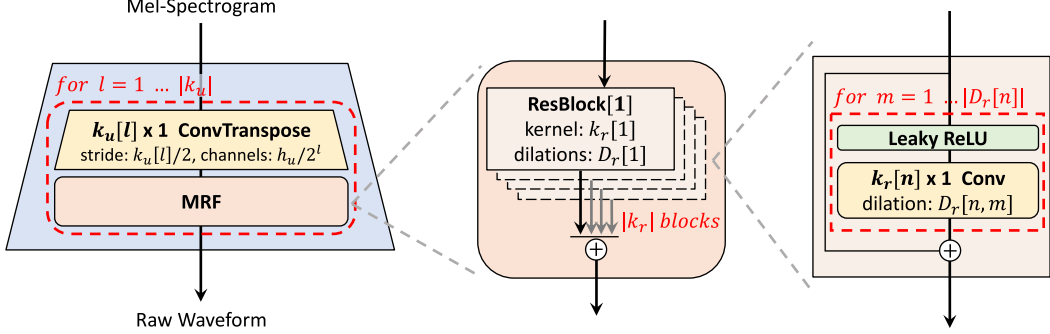


Figure 1: The generator upsamples mel-spectrograms up to  $|k_u|$  times to match the temporal resolution of raw waveforms. A MRF module adds features from  $|k_r|$  residual blocks of different kernel sizes and dilation rates. Lastly, the  $n$ -th residual block with kernel size  $k_r[n]$  and dilation rates  $D_r[n]$  in a MRF module is depicted.

of the generator. As in previous studies (Mathieu et al., 2015, Isola et al., 2017, Kumar et al., 2019), noise is not given to the generator as an additional input.

**Multi Receptive Field Fusion** We design a module for our generator, that observes patterns of various lengths in parallel. This is referred to as the multi receptive field fusion (MRF) module. Specifically, the MRF module returns the sum of outputs of multiple residual blocks. Different kernel sizes and dilation rates are selected for each residual block to form diverse receptive field patterns. The architectures of the MRF module and a residual block are shown in Figure 1. We left some adjustable parameters in the generator; the hidden dimension  $h_u$ , kernel sizes  $k_u$  of the transposed convolutions, kernel sizes  $k_r$ , and dilation rates  $D_r$  of the MRF modules can be regulated to satisfy one’s own requirement in a trade-off between synthesis efficiency and sample quality.

### 2.3 Discriminator

Identifying long-term dependencies is the key for modeling realistic speech audio. For example, a phoneme duration can be longer than 100 ms, resulting in high correlation between more than 2200 adjacent samples in the raw waveform. This problem has been addressed in the previous study (Donahue et al., 2018) by increasing receptive fields of the generator and discriminator. We focus on another crucial problem that has yet been resolved; as speech audio consists of sinusoidal signals with various periods, the diverse periodic patterns underlying in the audio data need to be identified.

To this end, we propose the multi-period discriminator (MPD) consisting of several sub-discriminators each handling a portion of periodic signals of input audio. Additionally, for capturing consecutive patterns and long-term dependencies, we use the multi-scale discriminator (MSD) proposed in MelGAN (Kumar et al., 2019), which consecutively evaluates audio samples at different levels.

**Multi-Period Discriminator** The MPD is a mixture of sub-discriminators, each of which only accepts equally spaced samples in an input audio; the space is given as period  $p$ . the sub-discriminators are designed to capture different implicit structures from each other by looking at different parts of an input audio. We set the periods to  $[2, 3, 5, 7, 11]$  to avoid overlaps as much as possible. As shown in Figure 2b, we first reshape 1D raw audio of length  $T$  into 2D data of height  $T/p$  and width  $p$  and then apply 2D convolutions to the reshaped data. In every convolutional layer of the MPD, we restrict the kernel size in the width axis to be 1 to process the periodic samples independently. Each sub-discriminator is a stack of strided convolutional layers with leaky rectified linear unit (ReLU) activation. Subsequently, weight normalization (Salimans and Kingma, 2016) is applied to the MPD. By reshaping the input audio into 2D data instead of sampling periodic signals of audio, gradients from the MPD can be delivered to all time steps of the input audio.

**Multi-Scale Discriminator** Because each sub-discriminator in the MPD only accepts disjoint samples, we add the MSD to consecutively evaluate the audio sequence. The architecture of the

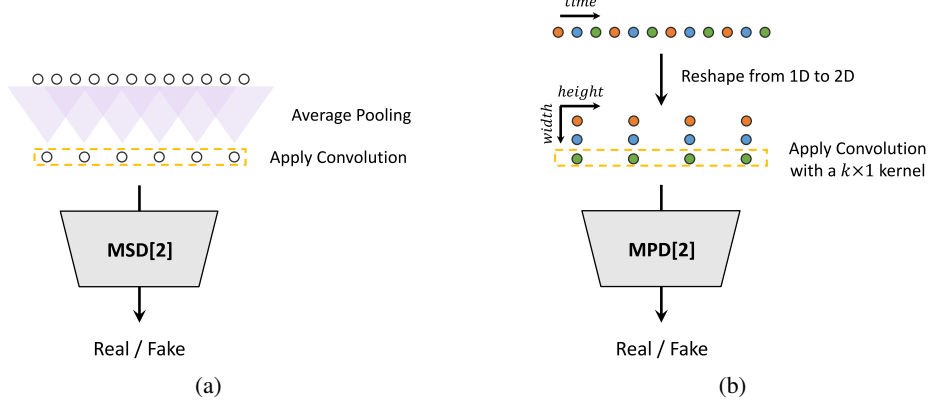


Figure 2: (a) The second sub-discriminator of the MSD. (b) The second sub-discriminator of the MPD with period 3.

MSD is drawn from that of MelGAN (Kumar et al., 2019). The MSD is a mixture of three sub-discriminators operating on different input scales: raw audio,  $\times 2$  average-pooled audio, and  $\times 4$  average-pooled audio, as shown in Figure 2a. Each of the sub-discriminators in the MSD is a stack of strided and grouped convolutional layers with leaky ReLU activation. The discriminator size is increased by reducing stride and adding more layers. Weight normalization is applied except for the first sub-discriminator, which operates on raw audio. Instead, spectral normalization (Miyato et al., 2018) is applied and stabilizes training as it reported.

Both the MPD and MSD are Markovian window-based discriminators (Kumar et al., 2019, Isola et al., 2017); they do not return one scalar value over an entire sequence, but return one scalar for each overlapping window of discriminators. Note that the MPD operates on disjoint samples of raw waveforms, whereas the MSD operates on smoothed waveforms.

## 2.4 Training Loss Terms

**GAN Loss** For brevity, we describe our discriminators, MSD and MPD, as one discriminator throughout Section 2.4. For the generator and discriminator, the training objectives follow LS-GAN (Mao et al., 2017), which replace the binary cross-entropy terms of the original GAN objectives (Goodfellow et al., 2014) with least squares loss functions for non-vanishing gradient flows. The discriminator is trained to classify ground truth samples, and the samples synthesized from the generator approximately equal to 1 and 0. The generator is trained to fake the discriminator by updating the sample quality to be classified to a value almost equal to 1. GAN losses for the generator  $G$  and the discriminator  $D$  are defined as

$$\mathcal{L}_{Adv}(D; G) = \mathbb{E}_{(x, s)} \left[ (D(x) - 1)^2 + (D(G(s)))^2 \right] \quad (1)$$

$$\mathcal{L}_{Adv}(G; D) = \mathbb{E}_s \left[ (D(G(s)) - 1)^2 \right] \quad (2)$$

, where  $x$  denotes the ground truth audio and  $s$  denotes the input condition, the mel-spectrogram of the ground truth audio.

**Mel-Spectrogram Loss** In addition to the GAN objective, we add a mel-spectrogram loss for stable and efficient training of the generator. The mel-spectrogram loss is the L1 distance between the mel-spectrogram of a waveform synthesized by the generator and that of a ground truth waveform. It is defined as

$$\mathcal{L}_{Mel}(G) = \mathbb{E}_{(x, s)} \left[ \|\phi(x) - \phi(G(s))\|_1 \right] \quad (3)$$

, where  $\phi$  is the function that transforms a waveform into the corresponding mel-spectrogram. The mel-spectrogram loss helps the generator to synthesize a waveform corresponding to an input condition, which stabilizes the adversarial training process from the early stages.

**Feature Matching Loss** The feature matching loss is a learned similarity metric measured by the difference in features of the discriminator between a ground truth sample and a generated sample (Larsen et al., 2015, Kumar et al., 2019). As it was successfully adopted to speech synthesis (Kumar et al., 2019), we use it as an additional loss to train the generator. Every intermediate feature of the discriminator is extracted, and the L1 distance between a ground truth sample and a conditionally generated sample in each feature space is calculated. The feature matching loss is defined as

$$\mathcal{L}_{FM}(G; D) = \mathbb{E}_{(x, s)} \left[ \sum_{i=1}^T \frac{1}{N_i} \|D^i(x) - D^i(G(s))\|_1 \right] \quad (4)$$

, where  $T$  denotes the number of layers in the discriminator;  $D^i$  and  $N_i$  denote the features and the number of features in the  $i$ -th layer of the discriminator, respectively.

**Final Loss** Our final objectives for the generator and discriminator are as

$$\mathcal{L}_G = \mathcal{L}_{Adv}(G; D) + \lambda_{fm} \mathcal{L}_{FM}(G; D) + \lambda_{mel} \mathcal{L}_{Mel}(G) \quad (5)$$

$$\mathcal{L}_D = \mathcal{L}_{Adv}(D; G) \quad (6)$$

, where we set  $\lambda_{fm} = 2$  and  $\lambda_{mel} = 45$ . Because our discriminator is a set of sub-discriminators of the MPD and MSD, Equations 5 and 6 can be converted with respect to the sub-discriminators as

$$\mathcal{L}_G = \sum_{k=1}^K \left[ \mathcal{L}_{Adv}(G; D_k) + \lambda_{fm} \mathcal{L}_{FM}(G; D_k) \right] + \lambda_{mel} \mathcal{L}_{Mel}(G) \quad (7)$$

$$\mathcal{L}_D = \sum_{k=1}^K \mathcal{L}_{Adv}(D_k; G) \quad (8)$$

, where  $D_k$  denotes the  $k$ -th sub-discriminator in the MPD and MSD.

### 3 Experiments

For fair and reproducible comparison with other models, we used the LJSpeech dataset (Ito, 2017) in which many speech synthesis models are trained. LJSpeech consists of 13,100 short audio clips of a single speaker with a total length of approximately 24 hours. The audio format is 16-bit PCM with a sample rate of 22 kHz; it was used without any manipulation. HiFi-GAN was compared against the best publicly available models: the popular mixture of logistics (MoL) WaveNet (Oord et al., 2017) implementation (Yamamoto, 2018) and the official implementation of WaveGlow (Valle, 2018b) and MelGAN (Kumar, 2019). We used the provided pretrained weights for all the models.

To evaluate the generality of HiFi-GAN to the mel-spectrogram inversion of unseen speakers, we used the VCTK multi-speaker dataset (Veaux et al., 2017), which consists of approximately 44,200 short audio clips uttered by 109 native English speakers with various accents. The total length of the audio clips is approximately 44 hours. The audio format is 16-bit PCM with a sample rate of 44 kHz. We reduced the sample rate to 22 kHz. We randomly selected nine speakers and excluded all their audio clips from the training set. We then trained MoL WaveNet, WaveGlow, and MelGAN with the same data settings; all the models were trained until 2.5M steps.

To evaluate the audio quality, we crowd-sourced 5-scale MOS tests via Amazon Mechanical Turk. The MOS scores were recorded with 95% confidence intervals (CI). Raters listened to the test samples randomly, where they were allowed to evaluate each audio sample once. All audio clips were normalized to prevent the influence of audio volume differences on the raters.

The synthesis speed was measured on GPU and CPU environments according to the recent research trends regarding the efficiency of neural networks (Kumar et al., 2019, Zhai et al., 2020, Tan et al., 2019). The devices used are a single NVIDIA V100 GPU and a MacBook Pro laptop (Intel i7

CPU 2.6GHz). Additionally, we used 32-bit floating point operations for all the models without any optimization methods.

To confirm the trade-off between synthesis efficiency and sample quality, we conducted experiments based on the three variations of the generator,  $V1$ ,  $V2$ , and  $V3$  while maintaining the same discriminator configuration. For  $V1$ , we set  $h_u = 512$ ,  $k_u = [16, 16, 4, 4]$ ,  $k_r = [3, 7, 11]$ , and  $D_r = [[1, 1, 3, 1, 5, 1] \times 3]$ .  $V2$  is simply a smaller version of  $V1$ , which has a smaller hidden dimension  $h_u = 128$  but with exactly the same receptive fields. To further reduce the number of layers while maintaining receptive fields wide, the kernel sizes and dilation rates of  $V3$  were selected carefully. The detailed configurations of the models are listed in the Appendix. We used 80 bands mel-spectrograms as input conditions. The FFT, window, and hop size were set to 1024, 1024, and 256, respectively. The networks were trained using the AdamW optimizer (Loshchilov and Hutter, 2017) with  $\beta_1 = 0.8$ ,  $\beta_2 = 0.99$ , and weight decay  $\lambda = 0.01$ . The learning rate decay was scheduled by a 0.999 factor in every epoch with an initial learning rate of  $2 \times 10^{-4}$ .

## 4 Results

### 4.1 Audio Quality and Synthesis Speed

To evaluate the performance of our models in terms of both quality and speed, we performed the MOS test and the speed measurement. For the MOS test, we randomly selected 50 utterances from the LJSpeech dataset, which were excluded in the training.

For easy comparison of audio quality, synthesis speed and model size, the results are compiled and presented in Table 1. Remarkably, all variations of HiFi-GAN scored higher than the other models.  $V1$  has 13.92M parameters and achieves the highest MOS score with a gap of 0.09, compared to the ground truth audio; this implies that the synthesized audio is nearly indistinguishable to the human voice. In terms of synthesis speed,  $V1$  is faster than WaveGlow and MoL WaveNet.  $V2$  also demonstrates similarity to human quality with a MOS score of 4.23 while significantly reducing the memory requirement and inference time, compared to  $V1$ . It only requires 0.92M parameters. Despite having the lowest MOS score among our models,  $V3$  can synthesize speech 13.44 times faster than real time on CPU and 1,186 times faster than real time on single V100 GPU while showing similar perceptual quality with the MoL WaveNet. Because  $V3$  efficiently synthesize speech on CPU, it can be well suited for on-device applications.

Table 1: Comparison of the MOS and the synthesis speed. Speed of  $n$  kHz means that the model can generate  $n \times 1000$  raw audio samples per second. The numbers in () mean the speed compared to real time.

Model	MOS (CI)	Speed on CPU (kHz)	Speed on GPU (kHz)	# Param (M)
Ground Truth	4.45 ( $\pm 0.06$ )	—	—	—
WaveNet (MoL)	4.02 ( $\pm 0.08$ )	—	0.07 ( $\times 0.003$ )	24.73
WaveGlow	3.81 ( $\pm 0.08$ )	4.72 ( $\times 0.21$ )	501 ( $\times 22.75$ )	87.73
MelGAN	3.79 ( $\pm 0.09$ )	145.52 ( $\times 6.59$ )	14,238 ( $\times 645.73$ )	4.26
HiFi-GAN $V1$	<b>4.36</b> ( $\pm 0.07$ )	31.74 ( $\times 1.43$ )	3,701 ( $\times 167.86$ )	13.92
HiFi-GAN $V2$	4.23 ( $\pm 0.07$ )	214.97 ( $\times 9.74$ )	16,863 ( $\times 764.80$ )	<b>0.92</b>
HiFi-GAN $V3$	4.05 ( $\pm 0.08$ )	<b>296.38</b> ( $\times 13.44$ )	<b>26,169</b> ( $\times 1,186.80$ )	1.46

### 4.2 Ablation Study

We performed an ablation study of the MPD, MRF, and mel-spectrogram loss to verify the effect of each HiFi-GAN component on the quality of the synthesized audio.  $V3$  was used as a generator for the ablation study, and the network parameters were updated up to 500k steps for each configuration.

The results of the MOS evaluation are shown in Table 2, which show all three components contribute to the performance. Removing the **MPD** causes a significant decrease in perceptual quality, whereas the absence of the **MSD** shows a relatively small but noticeable degradation. To investigate the effect

of the **MRF**, one residual block with the widest receptive field was retained in each MRF module. The result is also worse than the baseline. When the model was trained without the **mel-spectrogram loss**, the training process became unstable, and some pronunciations were synthesized differently from the ground truth audio.

Table 2: Ablation study results. Comparison of the effect of each component on the synthesis quality.

Model	MOS (CI)
Ground Truth	4.33 ( $\pm 0.06$ )
Baseline (HiFi-GAN V3)	4.13 ( $\pm 0.07$ )
w/o MPD	1.92 ( $\pm 0.10$ )
w/o MSD	3.88 ( $\pm 0.08$ )
w/o MRF	4.01 ( $\pm 0.07$ )
w/o Mel-Spectrogram Loss	3.44 ( $\pm 0.10$ )

### 4.3 Generalization to Unseen Speakers

We used 50 randomly selected utterances of nine unseen speakers in the VCTK dataset that were excluded in the training set for the MOS test. Table 3 shows the experimental results for the mel-spectrogram inversion of the unseen speakers. The three generator variations scored 3.77, 3.69, and 3.61. They were all better than AR and flow-based models, indicating that the proposed models generalize well to unseen speakers. Additionally, the tendency of difference in MOS scores of the proposed models is similar with the result shown in Section 4.1, which can be maintained across different datasets.

Table 3: Quality comparison of synthesized utterances for unseen speakers.

Model	MOS (CI)
Ground Truth	3.79 ( $\pm 0.07$ )
WaveNet (MoL)	3.52 ( $\pm 0.08$ )
WaveGlow	3.52 ( $\pm 0.08$ )
MelGAN	3.50 ( $\pm 0.08$ )
HiFi-GAN V1	<b>3.77</b> ( $\pm 0.07$ )
HiFi-GAN V2	3.69 ( $\pm 0.07$ )
HiFi-GAN V3	3.61 ( $\pm 0.07$ )

Table 4: Quality comparison for end-to-end speech synthesis.

Model	MOS (CI)
Ground Truth	4.23 ( $\pm 0.07$ )
WaveGlow (w/o fine-tuning)	3.69 ( $\pm 0.08$ )
HiFi-GAN V1 (w/o fine-tuning)	3.91 ( $\pm 0.08$ )
HiFi-GAN V2 (w/o fine-tuning)	3.88 ( $\pm 0.08$ )
HiFi-GAN V3 (w/o fine-tuning)	3.89 ( $\pm 0.08$ )
WaveGlow (find-tuned)	3.66 ( $\pm 0.08$ )
HiFi-GAN V1 (find-tuned)	<b>4.18</b> ( $\pm 0.08$ )
HiFi-GAN V2 (find-tuned)	4.12 ( $\pm 0.07$ )
HiFi-GAN V3 (find-tuned)	4.02 ( $\pm 0.08$ )

### 4.4 End-to-End Speech Synthesis

We conducted additional experiment to examine the effectiveness of the proposed models when applied to an end-to-end speech synthesis pipeline, which consists of *text to mel-spectrogram* and *mel-spectrogram to waveform* synthesis modules. We herein used Tacotron2 (Shen et al., 2018) to generate mel-spectrograms from text. Without any modification, we synthesized the mel-spectrograms using the most popular implementation of Tacotron2 (Valle, 2018a) with the provided pre-trained weights. We then fed them as input conditions into vocoders, including our models and WaveGlow used in Section 4.1.<sup>2</sup>

The MOS scores are listed in Table 4. The results without fine-tuning show that in the end-to-end setting, all the proposed models outperform WaveGlow, while the audio quality of all models are

<sup>2</sup> MelGAN and MoL WaveNet were excluded from comparison due to the difference of pre-processing such as frequency clipping. Since there was mismatch in the input representation, they both produced low quality audio when combined with Tacotron2.

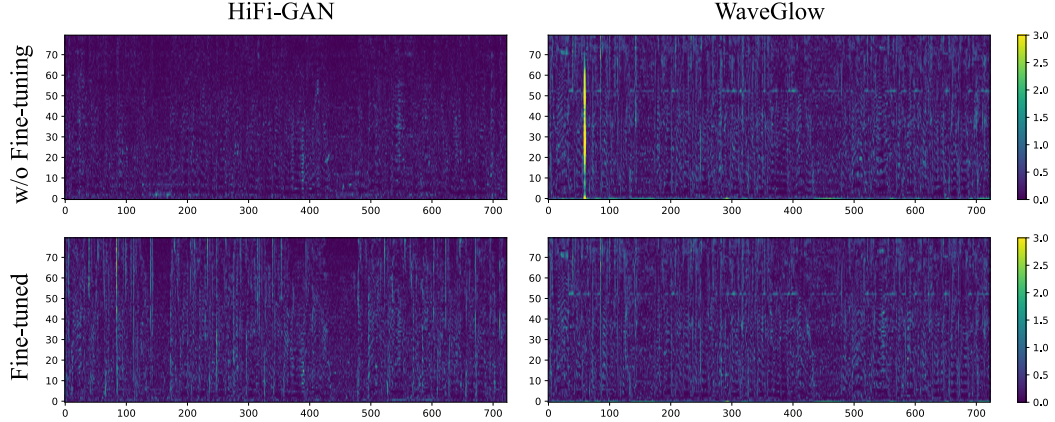


Figure 3: Pixel-wise difference in the mel-spectrogram domain between generated waveforms and a mel-spectrogram from Tacotron2. Before fine-tuning, HiFi-GAN generates waveforms corresponding to input conditions accurately. After fine-tuning, the error of the mel-spectrogram level increased, but the perceptual quality increased.

unsatisfactory compared to the ground truth audio. However, when the pixel-wise difference in the mel-spectrogram domain between generated waveforms and a mel-spectrogram from Tacotron2 are investigated as demonstrated in Figure 3, we found that the difference is insignificant, which means that the predicted mel-spectrogram from Tacotron2 was already noisy. To improve the audio quality in the end-to-end setting, we applied fine-tuning with predicted mel-spectrograms of Tacotron2 in teacher-forcing mode (Shen et al., 2018) to all the models up to 100k steps. MOS scores of all the fine-tuned proposed models over 4, whereas fine-tuned WaveGlow did not show quality improvement. We conclude that HiFi-GAN adapts well on the end-to-end setting with fine-tuning.

## 5 Conclusion

In this study, we introduced HiFi-GAN, which can efficiently synthesize high quality speech audio. Above all, our proposed model outperforms the best performing publicly available models in terms of synthesis quality, even comparable to human level. Moreover, it shows a significant improvement in terms of synthesis speed. We took inspiration from the characteristic of speech audio that consists of patterns with various periods and applied it to neural networks, and verified that the existence of the proposed discriminator greatly influences the quality of speech synthesis through the ablation study. Additionally, this study presented several experiments that are significant in speech synthesis applications. HiFi-GAN also generalizes well for speech synthesis of unseen speakers as well as an end-to-end setting. Remarkably, our small footprint model demonstrated comparable sample quality with the best publicly available autoregressive counterpart, while producing samples in an order-of-magnitude faster than real time on CPU. This shows progress towards on-device natural speech synthesis, which requires low latency and memory footprint. Finally, our experiments show that the generators of various configurations can be trained with the same discriminators and learning mechanism, which indicates the possibility of flexibly selecting a generator configuration according to the target specifications without the need for a time-consuming hyper-parameter search for the discriminators. HiFi-GAN will be released as open source, and we envisage that our work will serve as a basis for future speech synthesis studies.

## Acknowledgments

We would like to thank Bokyung Son, Sungwon Kim, Yongjin Cho and Sungwon Lyu.

## References

Mikołaj Bińkowski, Jeff Donahue, Sander Dieleman, Aidan Clark, Erich Elsen, Norman Casagrande, Luis C Cobo, and Karen Simonyan. High fidelity speech synthesis with adversarial networks. *arXiv preprint arXiv:1909.11646*, 2019.

Chris Donahue, Julian McAuley, and Miller Puckette. Adversarial audio synthesis. *arXiv preprint arXiv:1802.04208*, 2018.

Ian Goodfellow, Jean Pouget-Abadie, Mehdi Mirza, Bing Xu, David Warde-Farley, Sherjil Ozair, Aaron Courville, and Yoshua Bengio. Generative adversarial nets. In *Advances in neural information processing systems*, pages 2672–2680, 2014.

Phillip Isola, Jun-Yan Zhu, Tinghui Zhou, and Alexei A Efros. Image-to-image translation with conditional adversarial networks. In *Proceedings of the IEEE conference on computer vision and pattern recognition*, pages 1125–1134, 2017.

Keith Ito. The lj speech dataset. <https://keithito.com/LJ-Speech-Dataset/>, 2017.

Durk P Kingma and Prafulla Dhariwal. Glow: Generative flow with invertible 1x1 convolutions. In *Advances in Neural Information Processing Systems*, pages 10215–10224, 2018.

Kundan Kumar, Rithesh Kumar, Thibault de Boissiere, Lucas Gestin, Wei Zhen Teoh, Jose Sotelo, Alexandre de Brébisson, Yoshua Bengio, and Aaron C Courville. Melgan: Generative adversarial networks for conditional waveform synthesis. In *Advances in Neural Information Processing Systems 32*, pages 14910–14921, 2019.

Rithesh Kumar. descriptinc/melgan-neurips. <https://github.com/descriptinc/melgan-neurips>, 2019.

Anders Boesen Lindbo Larsen, Søren Kaae Sønderby, Hugo Larochelle, and Ole Winther. Autotencoding beyond pixels using a learned similarity metric. *arXiv preprint arXiv:1512.09300*, 2015.

Naihan Li, Shujie Liu, Yanqing Liu, Sheng Zhao, and Ming Liu. Neural speech synthesis with transformer network. In *Proceedings of the AAAI Conference on Artificial Intelligence*, volume 33, pages 6706–6713, 2019.

Ilya Loshchilov and Frank Hutter. Decoupled weight decay regularization. *arXiv preprint arXiv:1711.05101*, 2017.

Xudong Mao, Qing Li, Haoran Xie, Raymond YK Lau, Zhen Wang, and Stephen Paul Smolley. Least squares generative adversarial networks. In *Proceedings of the IEEE International Conference on Computer Vision*, pages 2794–2802, 2017.

Michael Mathieu, Camille Couprie, and Yann LeCun. Deep multi-scale video prediction beyond mean square error. *arXiv preprint arXiv:1511.05440*, 2015.

Takeru Miyato, Toshiki Kataoka, Masanori Koyama, and Yuichi Yoshida. Spectral normalization for generative adversarial networks. *arXiv preprint arXiv:1802.05957*, 2018.

Aaron van den Oord, Sander Dieleman, Heiga Zen, Karen Simonyan, Oriol Vinyals, Alex Graves, Nal Kalchbrenner, Andrew Senior, and Koray Kavukcuoglu. Wavenet: A generative model for raw audio. *arXiv preprint arXiv:1609.03499*, 2016.

Aaron van den Oord, Yazhe Li, Igor Babuschkin, Karen Simonyan, Oriol Vinyals, Koray Kavukcuoglu, George van den Driessche, Edward Lockhart, Luis C Cobo, Florian Stimberg, et al. Parallel wavenet: Fast high-fidelity speech synthesis. *arXiv preprint arXiv:1711.10433*, 2017.

Wei Ping, Kainan Peng, Andrew Gibiansky, Sercan O Arik, Ajay Kannan, Sharan Narang, Jonathan Raiman, and John Miller. Deep voice 3: Scaling text-to-speech with convolutional sequence learning. *arXiv preprint arXiv:1710.07654*, 2017.

Wei Ping, Kainan Peng, and Jitong Chen. Clarinet: Parallel wave generation in end-to-end text-to-speech. *arXiv preprint arXiv:1807.07281*, 2018.

Ryan Prenger, Rafael Valle, and Bryan Catanzaro. Waveglow: A flow-based generative network for speech synthesis. In *ICASSP 2019-2019 IEEE International Conference on Acoustics, Speech and Signal Processing (ICASSP)*, pages 3617–3621. IEEE, 2019.

Tim Salimans and Durk P Kingma. Weight normalization: A simple reparameterization to accelerate training of deep neural networks. In *Advances in neural information processing systems*, pages 901–909, 2016.

Jonathan Shen, Ruoming Pang, Ron J Weiss, Mike Schuster, Navdeep Jaitly, Zongheng Yang, Zhifeng Chen, Yu Zhang, Yuxuan Wang, Rj Skerrv-Ryan, et al. Natural tts synthesis by conditioning wavenet on mel spectrogram predictions. In *2018 IEEE International Conference on Acoustics, Speech and Signal Processing (ICASSP)*, pages 4779–4783. IEEE, 2018.

Mingxing Tan, Ruoming Pang, and Quoc V Le. Efficientdet: Scalable and efficient object detection. *arXiv preprint arXiv:1911.09070*, 2019.

Rafael Valle. Nvidia/tacotron2. <https://github.com/NVIDIA/tacotron2>, 2018a.

Rafael Valle. Nvidia/waveglow. <https://github.com/NVIDIA/waveglow>, 2018b.

Christophe Veaux, Junichi Yamagishi, Kirsten MacDonald, et al. Cstr vctk corpus: English multi-speaker corpus for cstr voice cloning toolkit. *University of Edinburgh. The Centre for Speech Technology Research (CSTR)*, 2017.

Ryuichi Yamamoto. wavenet vocoder. [https://github.com/r9y9/wavenet\\_vocoder/](https://github.com/r9y9/wavenet_vocoder/), 2018.

Ryuichi Yamamoto, Eunwoo Song, and Jae-Min Kim. Parallel wavegan: A fast waveform generation model based on generative adversarial networks with multi-resolution spectrogram. In *ICASSP 2020-2020 IEEE International Conference on Acoustics, Speech and Signal Processing (ICASSP)*, pages 6199–6203. IEEE, 2020.

Bohan Zhai, Tianren Gao, Flora Xue, Daniel Rothchild, Bichen Wu, Joseph E Gonzalez, and Kurt Keutzer. Squeezewave: Extremely lightweight vocoders for on-device speech synthesis. *arXiv preprint arXiv:2001.05685*, 2020.

## Appendix

### 1. Details of the Model Architecture

The detailed architecture of the generator and MPD is depicted in Figure 4. The configuration of three variants of the generator is listed in Table 5.

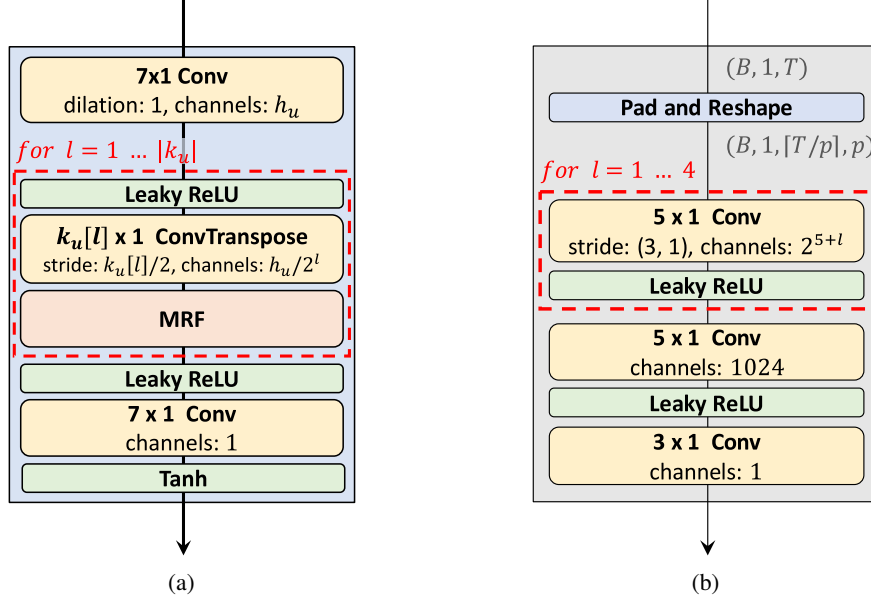


Figure 4: (a) The generator. (b) The sub-discriminator of the MPD with period  $p$ .

Table 5: Hyper-parameters of three generator  $V1$ ,  $V2$ , and  $V3$ .

Model	Hyper-Parameters			
	$h_u$	$k_u$	$k_r$	$D_r$
$V1$	512	[16, 16, 4, 4]	[3, 7, 11]	$[[1, 1], [3, 1], [5, 1]] \times 3$
$V2$	128	[16, 16, 4, 4]	[3, 7, 11]	$[[1, 1], [3, 1], [5, 1]] \times 3$
$V3$	256	[16, 16, 8]	[3, 5, 7]	$[[1], [2]], [[2], [6]], [[3], [12]]$

Each ResBlock in the generators is a structure in which multiple convolution layers and residual connections are stacked. In the ResBlock of  $V1$  and  $V2$ , 2 convolution layers and 1 residual connection are stacked 3 times. In the Resblock of  $V3$ , 1 convolution layer and 1 residual connection are stacked 2 times. Therefore,  $V3$  consists of a much smaller number of layers than  $V1$  and  $V2$ .